ACS SyntheticBiology

pubs.acs.org/synthbio Research Article

Highly Efficient Biosynthesis of Hypoxanthine in *Escherichia coli* and Transcriptome-Based Analysis of the Purine Metabolism

Min Liu, Yingxin Fu, Wenjie Gao, Mo Xian,* and Guang Zhao*

Cite This: *ACS Synth. Biol.* 2020, 9, 525−535 Read Online

ACCESS | Metrics & More | Article Recommendations | Supporting Information

ABSTRACT: Nucleosides and purine analogues have multiple functions in cell physiology, food additives, and pharmaceuticals, and some are produced on a large scale using different microorganisms. However, biosynthesis of purines is still lacking. In the present study, we engineered the *de novo* purine biosynthesis pathway, branched pathways, and a global regulator to ensure highly efficient hypoxanthine production by *Escherichia coli*. The engineered strain Q2973 produced 1243 mg/L hypoxanthine in fed-batch fermentation, accompanied by an extremely low accumulation of byproducts such as acetate and xanthine. We also performed global gene expression analysis to illustrate the mechanism for improving hypoxanthine production. This study demonstrated the feasibility of large-scale hypoxanthine production byan engineered *E. coli* strain, and provides a reference for subsequent studies on purine analogues and nucleosides.

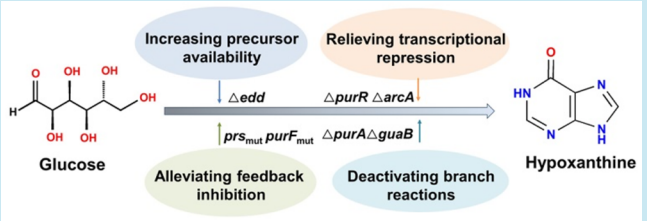

KEYWORDS: *hypoxanthine, metabolic engineering, transcriptome, Escherichia coli*

Purine intermediates comprising phosphorylated nucleotides, nucleosides, and nucleobases have multiple functions in cell physiology.[1,2] For example, they are the structural components of DNA and RNA, energy carriers, and enzyme cofactors, which subsequently serve as genetic information transmitters, phosphate group donors, and signal mediators.[3,4] Some purine intermediates also have secondary functions in food additives (regarding flavor and nutrition) and pharmaceuticals.[5] Hypoxanthine is a purine nucleobase, the derivatives of which have long been used in the pharmaceutical industry for research. The 6-hydroxyl group of hypoxanthine is highly active, and its derivatives (such as 6-mercaptopurine) are used as anticancer drugs and plant growth regulators. In addition, purine compounds can be used as inducers of interferon release, ligands of adrenocorticotropin receptors, and antagonists of adenosine receptor agonists.

Nucleosides and purine analogues have gained immense economic interest, particularly in pharmaceutical and biotechnological industries, and some of these compounds have been successfully synthesized in the past mainly by (1) microbial fermentation;[2,6,7] (2) RNA extraction and breakdown into free nucleotides and nucleosides; (3) excretion of nucleosides into the culture medium and further phosphorylation through chemical or enzymatic methods.[5] In recent years, the metabolic engineering approach has proven most efficient because of significant improvements in nucleoside production in different microorganisms.[8,9]

In most microorganisms, purine biosynthesis involves the *de novo* purine biosynthesis and salvage pathways. Between these, the former pathway is nearly ubiquitous and begins with simple substrates such as amino acids and bicarbonates. First, 5-phosphoribosyl-1-pyrophosphate (PRPP; an important intermediate) is converted to inosine monophosphate (IMP) via 10 sequential catalytic reactions. Then, IMP is transformed into adenosine monophosphate (AMP) or guanosine monophosphate (GMP) in two additional steps (Figure 1). In contrast, nucleotides are degraded into nucleosides and further degraded into nucleobases, which enter the salvage pathway through the action of nucleotidases.[10,11]

Nevertheless, some nucleosides and purine analogues of interest are difficult to accumulate in their natural state because of multiple layers of regulation such as transcriptional repression and feedback inhibition.[7] Studies have revealed that the purine repressor (PurR) can bind to operator sequences for the negative regulation of the expression of *pur* operon genes.[12,13] Hypoxanthine or guanine is a corepressor that induces a conformational change in PurR, inhibiting its transcription. Therefore, the environmental signal of excess purine, particularly of hypoxanthine or guanine, can induce the transcriptional repression of the *pur* operon with the help of PurR.[14,15]

The feedback inhibition of key enzymes should not be neglected in the *de novo* purine biosynthesis pathway. PRPP synthetase (Prs) is a link connecting the pentose phosphate (PP) pathway and *de novo* purine biosynthesis pathway. The

Received: September 29, 2019
Published: February 12, 2020

https://dx.doi.org/10.1021/acssynbio.9b00396
ACS Synth. Biol. 2020, 9, 525−535

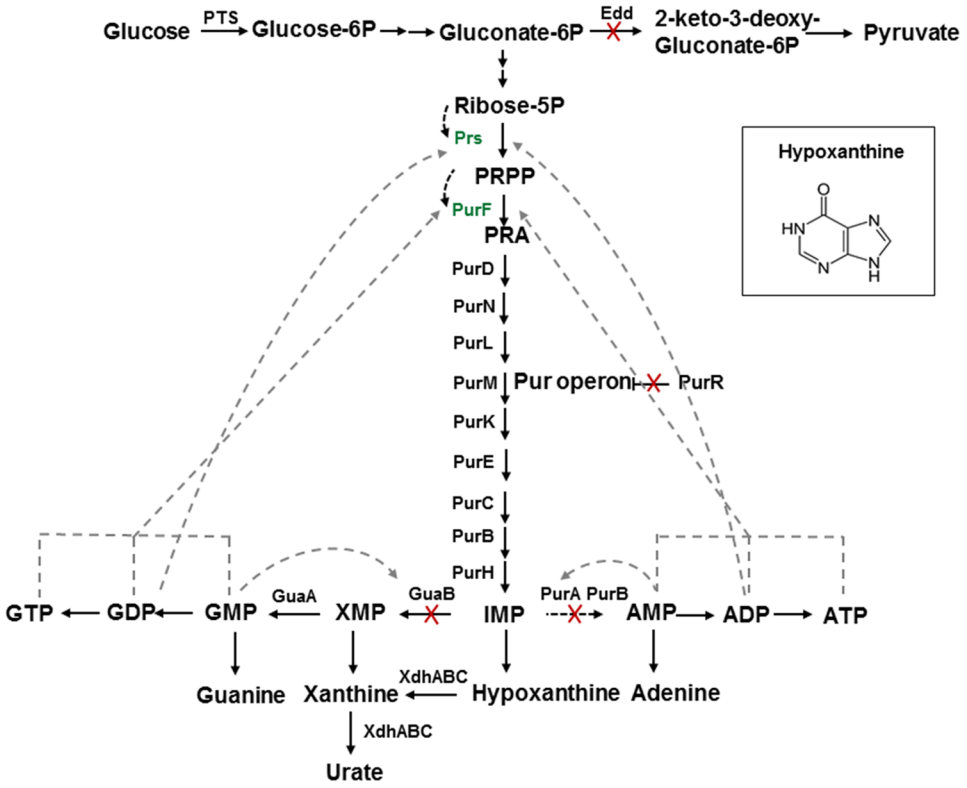

Figure 1. *De novo* purine biosynthesis pathway for hypoxanthine production from glucose in *E. coli*. Enzymes associated with reactions are shown, overexpressed genes are marked in red, and knockout genes are marked in green. Black solid lines represent metabolic conversions, black dotted lines depict enzyme activations, and gray dotted lines depict feedback inhibition. Abbreviations: PRPP, 5-phosphoribosyl-1-pyrophosphate; PRA, 5-phospho-α-D-ribosylamin; IMP, inosine 5′-monophosphate; XMP, xanthosine 5′-monophosphate; GMP, guanosine 5′-monophosphate; GDP, guanosine 5′-diphosphate; GTP, guanosine 5′-triphosphate; AMP, adenosine 5′-monophosphate; ADP, adenosine diphosphate; ATP, adenosine triphosphate; Prs: PRPP synthetase; PurF, PRPP amidotransferase; PurA, adenylosuccinate synthetase; PurB, adenylosuccinate lyase; GuaB, IMP dehydrogenase; GuaA, GMP synthase; XdhABC, xanthine dehydrogenase.

feedback inhibition of some nucleotides affects the enzyme activity of Prs, particularly of adenosine diphosphate (ADP) and guanosine diphosphate (GDP) (Figure 1).[9] Studies have shown that the substitution of D128 of Prs with A can desensitize feedback inhibition by ADP during inosine production in *E. coli*.[9] Moreover, PRPP amidotransferase (PurF) is the key regulatory enzyme that catalyzes the initial reaction in the *de novo* purine biosynthesis pathway.[16,17] PurF activity is repressed by purine nucleotides through feedback regulation.[18,19] Studies have reported that the amino acid replacements of K326Q and P410W in *E. coli* decrease its binding affinity for GMP and AMP and correspondingly reduce feedback inhibition.[9] To date, several researchers have produced nucleosides or their derivatives by metabolic engineering in *E. coli*, *Bacillus subtilis*, *Ashbya gossypii*, and *Corynebacterium glutamicum*. Among these microorganisms, *E. coli* certainly has been widely used for producing high-value chemicals and biofuels because of its rapid growth, ease of genetic manipulation, and low cost.[20]

In this study, we elucidated the possibility of large-scale hypoxanthine production in *E. coli* using metabolic engineering approaches related to the *de novo* purine biosynthesis pathway and central carbon metabolism including (1) relieving transcriptional repression, (2) alleviating feedback inhibition, (3) increasing precursor availability, and (4) deactivating branch reactions. An engineered *E. coli* strain Q2955 was generated, which accumulated 791.54 mg/L hypoxanthine in fed-batch fermentation. Remarkably, the byproducts acetate and xanthine were found accumulate in large amounts in Q2955. The global regulator ArcA is a component of the Arc system that regulates the expression of numerous operons under aerobic, microaerobic, and anaerobic conditions. Phosphorylated ArcA binds to the promoter region of downstream targets and regulates their expression.[21,22] In this study, we also successfully inhibited byproduct accumulation through an ArcA mutant. In addition, we performed transcriptome sequencing and quantitative RT-PCR analysis to illustrate the theoretical interpretation for improving hypoxanthine production.

RESULTS AND DISCUSSION

Regulation of the *de Novo* Purine Biosynthesis Pathway. In *E. coli*, the *de novo* purine biosynthesis pathway has been verified previously. *De novo* purine synthesis begins with the activation of the PP pathway intermediate and direct precursor ribose-5-phosphate, which is converted to IMP with concomitant consumption of 10 mol adenosine triphosphate (ATP).[23] In *E. coli*, the *pur* operon encodes the enzymes related to the *de novo* synthesis of IMP, which is arranged as individual loci and small polycistronic operons.[13] PurR is a member of the LacI/GalR family of transcriptional repressors.[14] To relieve transcriptional repression of the *pur* operon, we constructed a *purR*-deleted strain, that is, Q2794, via P_1 vir-mediated transduction following a method previously described.[24] After 48 h shake-flask cultivation, the hypoxanthine production by Q2794 in the culture medium was found

https://dx.doi.org/10.1021/acssynbio.9b00396
ACS Synth. Biol. 2020, 9, 525−535

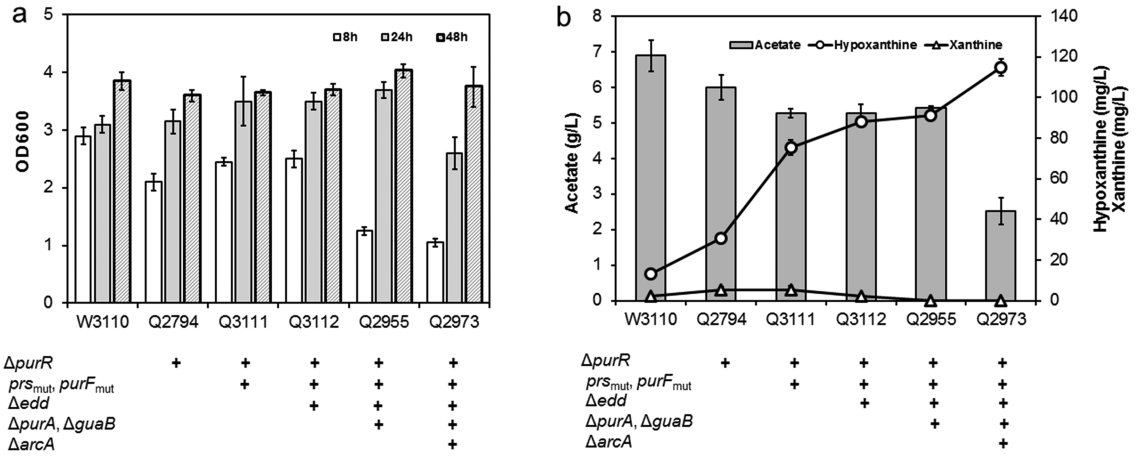

Figure 2. Growth (a) and the production of hypoxanthine, xanthine and acetate (b) of *E. coli* strains W3110, Q2791, Q3111, Q3112, Q2955, and Q2973 in shake-flask fermentation. Columns present the average of triplicate experiments, and error bars represent standard deviation.

to be 30.72 ± 0.93 mg/L, which was >2 times higher than that produced by WT W3110 of 13.21 ± 1.70 mg/L, and the productions of xanthine by Q2794 and WT W3110 in the culture medium were 5.42 ± 1.25 mg/L and 2.36 ± 0.21 mg/L, respectively (Figure 2). The optical density at a wavelength of 600 nm (OD_{600}) for the *purR* mutant and WT W3110 was very similar after 48 h fermentation, indicating that *purR* inactivation does not affect cell growth obviously.

Previous studies have observed endogenous and exogenous accumulation of nucleobases when *E. coli* cells enter the stationary phase.[25,26] Uracil and xanthine were excreted into the extracellular space of the cells, and other nucleobases (except minor amounts of hypoxanthine), nucleosides, and nucleotides (except cyclic AMP) were not detected in significant amounts in the culture medium. These results showed that xanthine is the dominating extracellular nucleobase, whereas hypoxanthine is extracellularly present only in minor concentrations. In our study, xanthine was not detected in the intracellular space; however, hypoxanthine was mainly detected in the culture medium, and extremely low amounts of hypoxanthine were found in the intracellular space of cells with perchloric acid extraction, which contradicts previous findings.[25,27] It remains unclear whether culture conditions or metabolic engineering affected the transport and orientation of nucleobases in cells. However, relieving the transcriptional repression of PurR clearly improved hypoxanthine production.

The feedback inhibition of Prs and PurF also affects the *de novo* purine biosynthesis pathway. Prs catalyzes PRPP synthesis by transferring the β,γ-pyrophosphate group of ATP to the C1 hydroxyl group of ribose-5-phosphate, whereas PurF catalyzes phosphoribosylamine production by transferring glutamine amide nitrogen to PRPP. The site-directed substitution of Prs and PurF can alleviate feedback inhibition.[9] On the basis of these findings, we constructed site-specific mutations in Prs (D128A) and PurF (K326Q and P410W) using a fast site-directed mutagenesis kit and obtained the recombinant plasmid pACYCDuet-*prs* (D128A)-*purF* (K326Q, p410W). This recombinant plasmid was transformed to Q2794, yielding the engineered strain Q3111, which was cultured with 20 g/L glucose as the sole carbon source under the same culture conditions as used for the previous strain. After cultivation, Q3111 produced 75.38 ± 3.62 mg/L hypoxanthine, which was approximately 6 and 2.5 times higher than those produced by WT W3110 and Q2794, respectively, and the production of xanthine by Q3111 was 5.33 ± 1.82 mg/L (Figure 2). Therefore, site-specific Prs and PurF mutations can alleviate feedback inhibition and improve hypoxanthine production. However, there was no significant change in xanthine production through these above genetic modifications.

Regulation of the *de novo* purine biosynthesis pathway by relieving the transcriptional repression of the *pur* operon and by alleviating the feedback inhibition of Prs and PurF clearly improved hypoxanthine production by 6-fold than that by WT W3110. However, it did not achieve the expected results. The hypoxanthine titer remained low, and acetate overflow was extremely severe during cultivation. Manipulating the carbon flux distribution might optimize hypoxanthine production.

Manipulation of Central Carbon Metabolism. PRPP, an intermediate product of the PP pathway, serves as a substrate in the *de novo* synthesis of purine nucleobases. The carbon glucose is first converted to gluconate-6P by sequential catalytic reactions in the PP pathway. Gluconate-6P is converted to PRPP for the *de novo* synthesis of purine nucleobases, while it is also catalyzed by the gluconate-6P dehydrogenase Edd for another reaction. To increase the PRPP substrate pool for purine nucleobase synthesis, *edd* inactivation was performed to weaken the branch metabolic flow. The genetic modification of *edd* deletion was incorporated into Q3111, yielding a new strain Q3112. Q3112 produced 88.20 ± 3.62 mg/L hypoxanthine, which is clearly higher than that produced by Q3111, and xanthine accumulation of Q3112 was only 2.16 ± 0.06 mg/L (Figure 2). These results suggested that increasing precursor availability by reducing branch competition contributes to the synthesis of hypoxanthine nucleobases.

In the *de novo* purine biosynthesis pathway, the substrate PRPP is first converted to IMP, which is the first compound with a complete purine ring in this pathway. Then, IMP is degraded to form the target compound hypoxanthine. However, the catalysis of specific enzymes can convert IMP to GMP or AMP (Figure 1). Therefore, deactivating IMP branch reactions might help in hypoxanthine accumulation. Considering this information, we simultaneously knocked out *guaB* and *purA* in Q3112, obtaining a new engineered strain, i.e., Q2955. The cell growth of Q2955 was obviously lower than that of the other strains in the early stage of fermentation, and the OD_{600} was only 1.25 ± 0.07 at 8 h fermentation.

https://dx.doi.org/10.1021/acssynbio.9b00396
ACS Synth. Biol. 2020, 9, 525−535

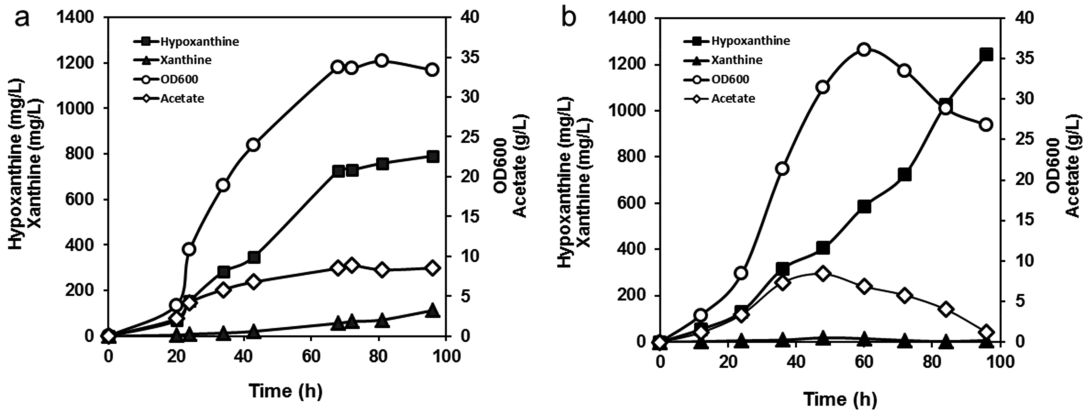

Figure 3. Time profiles for OD_{600} as well as hypoxanthine, xanthine, and acetate production by Q2955 (a) and Q2973 (b) in fed-batch fermentation. Culture was performed in a 5 L laboratory fermenter containing 2 L of fermentation medium.

However, the biomass of Q2955 was very similar to that of the other strains at 48 h fermentation. These results revealed that the blocked synthesis of GMP and AMP did not affect the final biomass accumulation, but retarded the cell growth in the early stage of cultivation. So, there are other replenishment pathways for the synthesis of GMP and AMP in *purA* and *guaB* knockout strains. The hypoxanthine production of Q2955 was 91.26 ± 3.62 mg/L, which was 6.91-fold higher than that of WT W3110 (Figure 2). The *de novo* purine biosynthesis pathway is regulated tightly by different mechanisms such as feedback inhibition of Prs and PurF. In addition, the two enzymes PurA and GuaB are under the feedback regulation of AMP and GMP, respectively.[7] We believe that PurA and GuaB are already tightly regulated in native cells; hence, PurA and GuaB knockout might have no obvious effects on hypoxanthine production.

To test the suitability of the engineered strains for large-scale hypoxanthine production, fed-batch fermentation was performed on the basis of shake-flask fermentation results. Because Q2955 showed a higher hypoxanthine titer than other strains, it was used in fed-batch fermentation in a 5 L laboratory fermenter. Cell growth as well as residual glucose, purine nucleobase, and acetate concentrations were monitored during cultivation. To prevent overflow metabolism, residual glucose concentrations in the culture were controlled below 2 g/L via automatic feeding of 60% (w/w) glucose. Figure 3a shows the time profiles of OD_{600} as well as hypoxanthine, xanthine, and acetate concentrations during the entire fermentation period; all these values increased gradually with time. After fermentation, the hypoxanthine titer of Q2955 was 791.54 mg/L. In addition, hypoxanthine can be converted to xanthine by catalysis of xanthine dehydrogenase (Xdh ABC) in the *de novo* purine biosynthesis pathway (Figure 1). Therefore, we monitored xanthine accumulation during the entire fermentation, and the final xanthine yield was found to be 112.43 mg/L. This suggests that xanthine dehydrogenase is a potential target for improving hypoxanthine accumulation.

Simultaneous regulation of the *de novo* purine biosynthesis pathway and central carbon metabolism significantly improved hypoxanthine production by Q2955 compared with that by WT W3110. However, acetate accumulation was still maintained at 8.53 g/L with controlling the glucose supply. Acetate overflow severely affects cell density, biomass accumulation, and synthesis of macromolecules (such as DNA, RNA, proteins, and lipids), even at a low concentration.[28,29] In central carbon metabolism, acetate was produced from pyruvate by pyruvate oxidase (PoxB) and from acetyl-coenzyme A (acetyl-CoA) by phosphotransacetylase−acetate kinase.[30] Acetate is distributed at about 10%−30% carbon flux from glucose as the sole carbon in aerobic fermentation.[29] There seems no direct relationship between the acetate metabolic pathway and *de novo* purine biosynthesis pathway, but the large acetate accumulation has adverse effects on cell activity and results in considerable unbeneficial carbon flux distribution. Therefore, redistributing the carbon flux globally might inhibit acetate overflow and improve hypoxanthine production and glucose conversion efficiency.

Redistribution of the Carbon Flux through a Global Regulator. Acetate overflow showed adverse effects on cell activity, glucose use, and formation of desired metabolites. Our previous study revealed that knockout of *arcA* gene was a solution to overcome acetate excretion and improve the production of the targets.[31] To redistribute the carbon flux, ArcA was deleted in Q2955, which resulted in a new engineered strain, that is, Q2973. The Arc system comprised ArcA and the membrane-bound sensor kinase ArcB.[21] ArcB is autophosphorylated at the expense of ATP and sequentially transfers the phosphoryl group to ArcA; phosphorylated ArcA controls the expression of numerous genes related to central carbon metabolic pathways such as the tricarboxylic acid (TCA) cycle, PP pathway, and glyoxylate cycle.[22,28] Q2973 was cultivated under the same culture conditions as Q2955 in shake-flask fermentation. The hypoxanthine titer increased to 114.75 ± 4.23 mg/L, whereas the acetate titer decreased to 2.52 ± 0.37 g/L (Figure 2). The acetate excretion decreased by >64%. These results indicated that redistributing the carbon flux via inactivating the global regulator ArcA contributed to the improved hypoxanthine production and the decreased acetate accumulation. For hypoxanthine production, we used Q2973 in fed-batch fermentation in a 5 L laboratory fermenter. In the bioreactor, Q2973 produced 1243 mg/L hypoxanthine, which was a 1.57-fold improvement over Q2955 (Figure 3b). In addition, while hypoxanthine production was significantly higher by Q2973 than by Q2955 in shake-flask and fed-batch fermentation, xanthine and acetate concentration was extremely lower for Q2973. The xanthine concentration was constantly <20 mg/L during the entire fermentation. During the later stage of fermentation, the xanthine concentration decreased to approximately 6 mg/L, whereas the acetate concentration increased to 8.40 g/L at 48 h following

https://dx.doi.org/10.1021/acssynbio.9b00396
ACS Synth. Biol. 2020, 9, 525−535

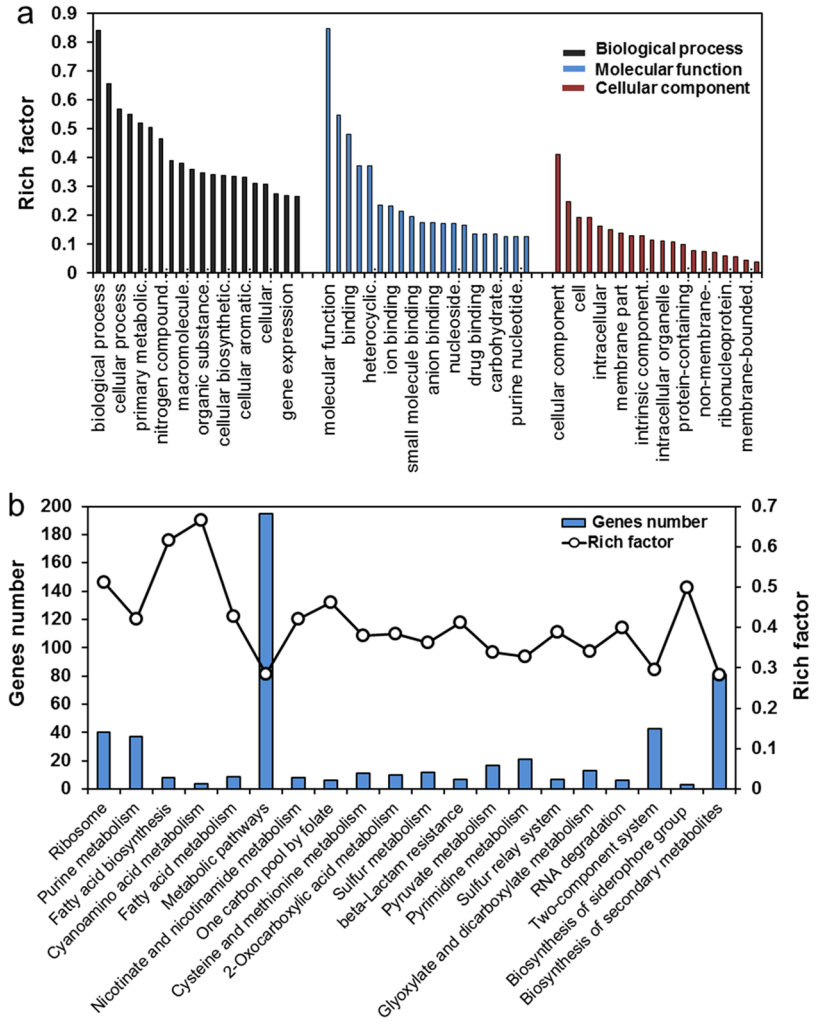

Figure 4. GO and KEGG pathway enrichment analysis of DEGs between Q2973 and WT W3110. (a) Distribution of GO terms for biological processes, molecular functions, and cellular components assigned to DEGs between Q2973 and WT W3100. (b) KEGG pathway enrichment analysis of DEGs between Q2973 and WT W3100. Gene number, number of DEGs in the pathway; Rich factor, ratio of DEGs annotated genes in a GO term or a KEGG pathway.

fermentation and then dropped to 1.21 g/L at the end of fermentation. Therefore, the ArcA mutant might decrease xanthine and acetate production by globally redistributing the carbon flux. The ArcA mutant can elevate the activities of the TCA cycle and glyoxylate pathway, and the latter one is the main pathway for acetate assimilation.[32,33] In the present study, *arcA* knockout probably activated the glyoxylate cycle and promoted more conversion from acetate to acetyl-CoA, which further entered the TCA cycle, yielding energy and important metabolites for cell activity. Therefore, a large amount of acetate accumulates in Q2973 during the early stage of fermentation, which can be assimilated during the later stage of fermentation, leading to lower acetate accumulation than that in Q2955. This might be why acetate excretion of the ArcA mutant decreases and hypoxanthine production increases.

In conclusion, we engineered an *E. coli* strain Q2973 and achieved the first efficient synthesis of hypoxanthine. Q2973 has the capacity for large-scale hypoxanthine production and has wide industrial application.

Transcriptome-Based Regulatory Mechanism Analysis. To determine the mechanism underlying enhanced hypoxanthine production, we conducted transcriptome sequencing and annotation to clarify the differences in the *de novo* purine biosynthesis pathway and central carbon metabolic pathways between Q2973 and WT W3110. The complementary DNA libraries of Q2973 and WT W3110 were submitted for high-throughput sequencing, and the generated sequencing reads were used to assemble the transcriptome of *E. coli*. Significant differentially expressed genes (DEGs) were analyzed by the enrichment of gene ontology (GO) and Kyoto Encyclopedia of Genes and Genomes (KEGG). Figure S1a in the Supporting Information shows the gene expression profile through Venn diagram analysis. The number of genes both expressed in Q2973 and WT W3110 was 3761. The percentage of 4.67% and 2.32% of genes was only detected in Q2973 and W3110, respectively, whereas the number of DEGs determined between these samples was 1206; among them, 583 were upregulated and 623 were downregulated (Figure S1b).

We have also discussed the distribution of GO terms for biological processes, molecular functions, and cellular components assigned to DEGs (Figure 4a). Among these, the GO terms for biological processes showed the most significant differences. The Rich factor was calculated as the ratio of DEGs to all genes annotated in a GO term or a KEGG

https://dx.doi.org/10.1021/acssynbio.9b00396
ACS Synth. Biol. 2020, 9, 525−535

pathway. The rich factors of GO terms above 0.5 mainly listed six, including the biological process, metabolic process, cellular process, organic substance metabolic process, primary metabolic process, and cellular metabolic process. The Rich factor related to functional description in GO terms was the highest for biological processes (0.841) and molecular functions (0.845).

All unigenes were assigned with KEGG orthology identifiers using the KEGG Automatic Annotation Server to interpret the major biochemical pathways and signal transduction involved in the *de novo* purine biosynthesis pathways and central carbon metabolism (Figure 4b). According to the KEGG enrichment analysis of DEGs, the metabolic pathways with significant differences included ribosomes, purine metabolism, fatty acid biosynthesis, and fatty acid metabolism. The Rich factors for all these pathways were >0.4. DEGs in the purine metabolic pathway were probably the direct reason for improved hypoxanthine production by Q2973. Table 2 and Figure 5 showed the annotations of different unigenes related to purine biosynthesis. Almost all genes in the *pur* operon, such as *purF*, *purC*, *purH*, and *purE*, were upregulated by 15-fold in Q2973 compared with those in WT W3110, whereas *purA* and *guaB* were downregulated by 10.9-fold and 22.9-fold, respectively. PurR deletion could increase gene transcription level in the *de novo* purine biosynthesis pathway and improve hypoxanthine production.

The IMP−XMP branched pathways catalyzed by GuaB and IMP−AMP branched pathways catalyzed by PurA were significantly downregulated, which further increased the carbon flux to hypoxanthine from the common precursor IMP (Figure 5). In Q2973, *edd* showed the most obvious variation in the gene transcription profile, and its expression was downregulated by 344.5-fold (Table 2). *edd* downregulation inevitably increased the PRPP substrate pool for *de novo* purine synthesis. The deletions of *purR*, *edd*, *purA*, *guaB*, and *arcA* led to downregulations instead of no-reads in the transcriptome analysis. We speculated that only the coding region of the gene was knocked out, and the low reads might come from the upstream or downstream noncoding region, which were assumed as the reads of the target gene during the sequencing data assembly.

In fed-batch fermentation, hypoxanthine production by Q2973 improved as well as xanthine and acetate accumulation was significantly lower compared with those in Q2955 (Figure 3). These results indicated that ArcA might globally redistribute the carbon flux to decrease the branch flux of byproducts. Transcriptome-based analysis showed that *arcA* knockout significantly improved the gene expression of isocitrate lyase (encoded by *aceA*) and malate synthase A (encoded by *aceB*) of the glyoxylate cycle (Table 2). The expression of *aceA* and *aceB* improved by >4-fold. In the glyoxylate cycle, isocitrate is directly split into succinate and glyoxylate by AceA catalysis without CO_2 loss, and the upregulation of this pathway might contribute to improved glucose conversion efficiency. Meanwhile, the glyoxylate cycle is the main pathway for acetate assimilation. *arcA* knockout activates this cycle and promotes acetate conversion to acetyl-CoA. This might be the reason for the significant acetate assimilation during the later stage of fermentation, leading to less acetate production by Q2973 compared with that by Q2955. However, we found no significant variation in the gene transcription profile of xanthine dehydrogenase, which was encoded by *xdhABC*, although we detected less xanthine accumulation in Q2973. The underlying mechanism needs further investigation.

Table 1. Plasmids and Strains Used in This Study

plasmids and strains	description	source
	Plasmids	
pACYCDuet1	Cm^r $oriP_{15A}$ $lacI^q$ T_7p	Novagen
pCP20	Cm^r, Amp^r pSC101 *oriCI857*	Novagen
pACYCDuet1-*prs* (D128A)	Cm^r $oriP_{15A}$ $lacI^q$ P_{prs} *prs*(D128A)	this study
pACYCDuet1-*purF* (K326Q)	Cm^r $oriP_{15A}$ $lacI^q$ $P_{lac,1-6}$ *purF* (K326Q)	this study
pACYCDuet1-*purF* (K326Q, P410W)	Cm^r $oriP_{15A}$ $lacI^q$ $P_{lac,1-6}$ *purF* (K326Q, P410W)	this study
pACYCDuet1-*prs* (D128A)-*purF* (K326Q, p410W)	Cm^r $oriP_{15A}$ $lacI^q$ P_{prs} *prs*(D128A) $P_{lac,1-6}$ *purF* (K326Q, P410W)	this study
	Strains	
E. coli DH5α	F^- *supE*44 Δ*lacU*169 (ϕ80 *lacZ* Δ*M15*) *hsdR*17 *recA*1 *endA*1 *gyrA*96 *thi*-1 *relA*1	Invitrogen
E. coli W3110	F^- λ^- rph-1 INV(rrnD, rrnE)	Invitrogen
JW1650	*E. coli* BW25113 *purR*::*kan*	Keio collection
JW1840	*E. coli* BW25113 *edd*::*kan*	Keio collection
JW4135	*E. coli* BW25113 *purA*::*kan*	Keio collection
JW5401	*E. coli* BW25113 *guaB*::*kan*	Keio collection
JW4364	*E. coli* BW25113 *arcA*::*kan*	Keio collection
Q2793	*E. coli* W3110 *purR*::*kan*	this study
Q2794	*E. coli* W3110△*purR*	this study
Q3111	*E. coli* W3110△ *purR*/ pACYCDuet-*prs* (D128A)-*purF* (K326Q, p410W)	this study
Q2828	*E. coli* W3110△*purR edd*::*kan*	this study
Q2850	*E. coli* W3110△*purR*△*edd*	this study
Q3112	*E. coli* W3110△ *purR*△*edd* / pACYCDuet-*prs* (D128A)-*purF* (K326Q, p410W)	this study
Q2895	*E. coli* W3110△*purR*△*edd purA*::*kan*	this study
Q2905	*E. coli* W3110△*purR*△*edd* △*purA*	this study
Q2913	*E. coli* W3110△*purR*△*edd* △*purA guaB*::*kan*	this study
Q2928	*E. coli* W3110△*purR*△*edd* △*purA* △*guaB*	this study
Q2955	*E. coli* W3110△*purR*△*edd* △*purA* △*guaB*/ pACYCDuet-*prs* (D128A)-*purF* (K326Q, p410W)	this study
Q2972	*E. coli* W3110△*purR*△*edd* △*purA* △*guaB arcA*::*kan*	this study
Q2973	*E. coli* W3110△*purR*△*edd* △*purA* △*guaB arcA*::*kan*/ pACYCDuet-*prs* (D128A)-*purF* (K326Q, p410W)	this study

Transcriptional Regulatory Analysis of PurR and ArcA by Quantitative RT-PCR. Transcriptome-based analysis showed that almost all genes in *pur* operon and many genes in central metabolism pathways of Q2973 were upreguated. To determine the transcriptional regulation of PurR and ArcA on the *pur* operon and central metabolism genes, total RNAs of WT W3110, Q2794, Q2955, and Q2973 were extracted for quantitative RT-PCR (qRT-PCR) analysis. The results showed that expression of *pur* operon genes in PurR mutant were upregulated, whereas *purR* deletion had no obvious effects on the expression of central metabolism genes, such as the TCA cylcle, glyoxylate pathway, and pentose phosphate pathway (Figure 6a). The transcription levels of *pur* operon and central metabolism genes in *arcA* mutant were upregulated at a different degree (Figure 6b). Among them, the gene expression

https://dx.doi.org/10.1021/acssynbio.9b00396
ACS Synth. Biol. 2020, 9, 525−535

Table 2. Annotation of Significantly Different Unigenes Related to Purine Biosynthesis in Hypoxanthine Producing Strain Q2973 versus Wild Type *E. coli* W3110

gene ID	readcount Q2973	readcount W3110	$\log_2$ (fold change)	*P* value	function
Up-Regulated Genes					
purF	477.78	17.40	4.56	6.12×10^{-09}	amidophosph oribosyltransferase
purC	83.59	5.35	3.88	4.11×10^{-08}	phosphoribosylaminoimidazole-succinocarboxamide synthase
purH	117.61	6.78	3.71	9.73×10^{-07}	Bifunctional phosphoribosylaminoimidazolecarboxamide formyltransferase/IMP cyclohydrolase cyclohydrolase
purE	25.14	1.65	3.52	2.48×10^{-08}	5-(carboxyamino)imidazole ribonucleotide mutase
purD	70.37	11.76	2.50	3.35×10^{-04}	phosphoribosylamine-glycine ligase
purM	25.25	4.95	2.32	2.27×10^{-04}	phosphoribosylformylglycinamidine cyclo-ligase
deoD	74.69	17.77	2.25	6.92×10^{-03}	purine-nucleoside phosphorylase
aceA	425.99	90.79	2.23	1.50×10^{-03}	isocitrate lyase
gmk	309.18	41.08	2.18	3.38×10^{-03}	guanylate kinase
aceB	610.85	145.68	2.04	1.42×10^{-02}	malate synthase A
nrdB	24.55	6.34	1.91	1.14×10^{-03}	ribonucleotide-diphosphate reductase subunit beta beta
purK	25.14	6.89	1.77	2.66×10^{-03}	5-(carboxyamino)imidazole ribonucleotide synthase
purN	10.19	2.02	1.68	8.73×10^{-03}	phosphoribosylglycinamide formyltransferase
purB	23.49	6.96	1.64	9.69×10^{-03}	adenylosuccinate lyase
purL	268.85	85.61	1.63	2.06×10^{-02}	phosphoribosylformylglycinamidine synthase
purU	30.27	9.49	1.61	4.75×10^{-03}	formyltetrahydrofolate deformylase
amn	31.33	10.77	1.58	8.30×10^{-03}	AMP nucleosidase
Down-Regulated Genes					
edd	0.11	37.92	−7.80	3.07×10^{-17}	phosphogluconate dehydratase
guaB	2.93	67.23	−4.97	3.28×10^{-11}	IMP dehydrogenase
purA	53.65	584.15	−3.91	4.92×10^{-07}	adenylosuccinate synthase
purR	15.43	118.70	−3.36	1.22×10^{-06}	HTH-type transcriptional repressor PurR
arcA	376.06	3565.71	−3.13	8.66×10^{-04}	two-component system response regulator ArcA regulator
atpC	31.22	244.44	−2.96	2.70×10^{-05}	F0F1 ATP synthase subunit epsilon subunit
apt	6.93	45.43	−2.91	9.46×10^{-07}	adenine phosphoribosyltransferase
atpD	77.73	404.95	−2.28	3.08×10^{-03}	F0F1 ATP synthase subunit beta
atpA	79.46	291.03	−1.82	1.46×10^{-02}	F0F1 ATP synthase subunit alpha subunit
atpF	26.24	68.87	−1.51	2.59×10^{-02}	ATP synthase Fo complex subunit

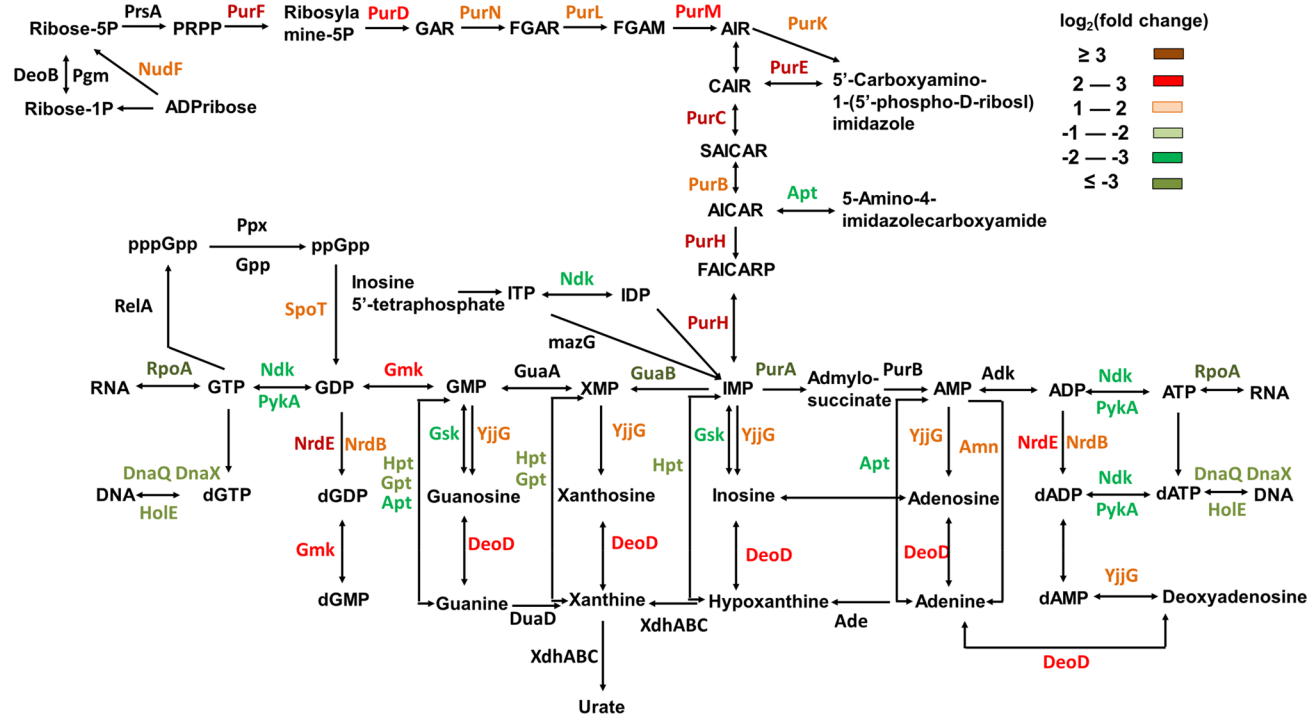

Figure 5. Unigene transcript expression changes related to the *de novo* purine biosynthesis pathway of Q2973 compared with that of WT W3110. Red marked, upregulated genes; green marked, downregulated genes.

https://dx.doi.org/10.1021/acssynbio.9b00396
ACS Synth. Biol. 2020, 9, 525−535

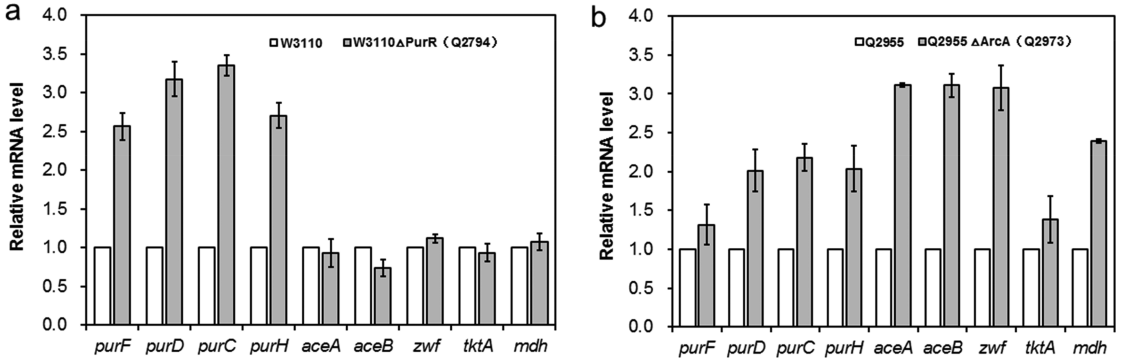

Figure 6. Transcriptional regulation analysis of PurR (a) and ArcA (b) on the *pur* operon and central metabolism genes by quantitative RT-PCR.

level of *purF* in Q2973 was only improved by 1.31-fold, and other *pur* operons genes, such as *purD*, *purC*, and *purH* were all regulated by more than two-folds. This may be caused by overexpression of *purF* (K326Q and P410W) in both Q2955 and Q2973, leading to an inconspicuous difference of *purF* transcription level in qRT-PCR experiment.

In *E. coli*, PurR is a transcriptional repressor that inhibits the genes expression of *pur* operon.[14] Knockout of *purR* indeed improved the genes transcription level of *pur* operon, conformed by transcriptome and qRT-PCR experiments, and further promoted the *de novo* biosynthesis of hypoxanthine. Some previous studies have demonstrated that knockout of *arcA* upregulated the expression of numerous genes related to central carbon metabolic pathways.[22,28] However, we found that *pur* operon was also regulated by the global regulator ArcA by qRT-PCR analysis. These results indicated that knockout of *arcA* might not only globally redistribute the carbon flux to decrease the branch flux of byproducts, but also directly improve the de novo biosynthesis of hypoxanthine. It enriched our understanding of the transcriptional regulation of ArcA, and presented application potential in the biosynthesis of the purine analogues and nucleosides.

CONCLUSIONS

In the present study, a strain of *E. coli*, that is, Q2973, was engineered for hypoxanthine production by manipulation of the *de novo* purine biosynthesis pathway and the main carbon metabolism pathways, and the redistributions of the carbon flux globally. Q2973 strain produced 1243 mg/L hypoxanthine with extremely low accumulation of byproducts in fed-batch fermentation. To the best of our knowledge, this is the first report on the successful hypoxanthine production in *E. coli*. In addition, transcriptome-based analysis was carried out to clarify the mechanism for improving hypoxanthine production. The upregulation of genes in the *pur* operon, the downregulation of IMP−XMP and IMP−AMP branch pathways, and the increase in the PRPP substrate pool might be the reasons for improved hypoxanthine production. In sum, we established the highly efficient biosynthesis of hypoxanthine, and this study provides a reference for subsequent studies on purine analogues and nucleosides.

MATERIAL AND METHODS

Plasmids and Strains Construction. Primers used in this study were listed in Table S1, plasmids and strains used in this study were listed in Table 1. *E. coli* DH5α was used for gene cloning and *E. coli* W3110 was used as the parent for all strain engineering. The site-directed mutagenesis for Prs and PurF wase performed using the fast site-directed mutagenesis kit (TianGen, China) following the manufacturer's instruction. The double mutant of *purF* (K326Q, P410W) containing a constitutive promoter $P_{lac,1-6}$ was cloned into pACYCDuet1 vector between *Sac*I, *Hind*III sites to generate a plasmid pACYCDuet1-*purF* (K326Q, P410W). Then, the singe mutant of *prs* (D128A) containing its native promoter was cloned into the recombinant plasmid pACYCDuet1-*purF* (K326Q, P410W) between *Bam*HI, *Sac*I sites to generate a new plasmid pACYCDuet1-*prs* (D128A)-*purF* (K326Q, p410W). The gene sequence and the intensity of transcription of $P_{lac,1-6}$ was showed in ref 34.

The chromosomal *purR*, *edd*, *purA*, *guaB*, and *arcA* genes of *E. coli* W3110 strain encoded for purine repressor, gluconate −6P dehydrogenase, adenylosuccinate synthetase, inosine 5′-monophosphate dehydrogenase and DNA-binding transcriptional dual regulator were knocked out via P_1 vir-mediated transduction as previously described.[24] The donor strain JW1650, JW1840, JW4135, JW5401, and JW4364 were from the Keio collection.[35] The recombinant plasmid was transformed to the corresponding hosts for the hypoxanthine biosynthesis.

Shake-Flask Cultivation. To evaluate the ability of hypoxanthine production in different engineered strains, shake-flask experiments were carried out in triplicate series of 250 mL Erlenmeyer flasks containing appropriate antibiotics. *E. coli* strains were grown overnight at 37 °C with shaking in LB broth, and then 1:50 diluted into 50 mL fresh LB broth with 20 g/L glucose. The culture was cultivated 48 h at 37 °C for hypoxanthine production. The OD_{600}, as well as hypoxanthine, xanthine, and acetate concentrations were detected after cultivation.

Fed-Batch Fermentation. To obtain higher hypoxanthine concentrations, fed-batch cultures were performed in a Biostat B plus MO5L fermentor (Sartorius, Germany) containing 2 L of LB broth medium. The culture medium was sterilized at 121 °C for 30 min. The glucose was filter-sterilized separately and added prior to initiate the fermentation. The seed culture was cultivated overnight at 37 °C in shake flasks containing 50 mL of LB liquid medium. The seed culture was then transferred into 2 L of LB broth medium with 20 g/L glucose and cultivated 96 h for hypoxanthine production. When the 20 g/L initial xylose was deleted, 60% (w/w) xylose began to be fed into the fermentor to maintain the residual xylose below 2 g/L. The pH was controlled about 7.0 via automatic addition of 10% (w/w) H_2SO_4 and 25% (w/w) ammonia−water during the whole fermentation. During the fermentation process, continuous sterile air was supplied at a flow rate of 2 L/min

https://dx.doi.org/10.1021/acssynbio.9b00396
ACS Synth. Biol. 2020, 9, 525−535

and the temperature was controlled at 37 °C. The dissolved oxygen (DO) level was maintained at 20 ± 1% by automatically adjusting stirring rate from 400 to 800 rpm. Antifoam was added to prevent frothing if necessary. Samples of the fermentation broth were removed at appropriate intervals to determine the $OD_{600,}$ as well as hypoxanthine, xanthine, and acetate concentrations during the entire fermentation period.

Analytic Methods. Culture samples were taken at several times throughout the experiments. The cell concentration was assayed by measuring optical density of the culture at 600 nm Cary 50 UV−vis, Varian). Metabolites in the culture supernatant were analyzed by LC−MS/MS analysis. To alleviate the contamination and damage of nonvolatile salts to the MS machine, the mobile phase before 1.2 min was injected into waste liquid. HPLC separation was carried out using a Thermo Acclaim RSLC C_{18} column (2.1 mm × 100 mm, 2.2 μm). All separations were performed at 30 °C with a constant flow rate of 200 μL/min using an Ultimate 3000 UHPLC (Thermo, USA). The autosample temperature was set to room temperature, and the injection volume was 2 μL. The mobile phase A consisted of 0.1% of formic acid in water, and the mobile phase B was composed of acetonitrile with 0.1% formic acid. A isocratic elution in 2% B was applied for sample separation in 10 min. A Compact Q-TOF mass spectrometry (Bruker Daltonics, Billerica, USA) with an ESI source in positive ion mode was used for MS analysis, using the following operation parameters: capillary voltage, 4500 V; dry temperature, 200 °C; nebulizing gas of 1.5 bar; drying gas (N_2, purity 99.999%) flow at 5.5 L/min. High resolution MS and MS/MS spectra were acquired in the range 50−1300 m/z. The collision gas was high purity nitrogen (purity 99.999%). The data were collected by auto MS/MS acquisition with a MS scan rate of 1 spectra/s and MS/MS scan rate of three precursor was acquired per cycle, active exclusion after 3 spectra and 1.0 min. Otof Control software was used to carry out mass spectrometer control and data acquisition and Compass Data Analysis Soft was applied for data analysis.

RNA Extraction and cDNA Library Construction. Total RNA was extracted using the mirVana miRNA Isolation Kit (Ambion) in accordance with the manufacturer's protocol. RNA integrity was assessed using the RNA Nano 6000 Assay Kit of the Bioanalyzer 2100 system (Agilent Technologies, CA, USA). A total amount of 3 μg of RNA per sample was used as input material for the RNA sample preparations. Sequencing libraries were generated using NEBNext UltraTM RNA Library Prep Kit for Illumina (NEB, USA) following manufacturer's recommendations, and index codes were added to attribute sequences to each sample.

Sequencing was performed at Beijing Novogene Bioinformatics Technology Co., Ltd. The raw sequence data were filtered by removing reads containing adapter, reads containing poly-N, and low-quality reads. The clean reads were aligned with the genome of *Escherichia coli* W3110. Gene expression was quantified as reads per kilobase of coding sequence per million reads (RPKM) algorithm.

Sequence Assembly and Annotation. Differential expression analysis of the engineering stain Q2973 and wild type W3110 was performed using the DESeq2 R package (1.16.1) . Genes with an adjusted P value < 0.05 found by DESeq were assigned as differentially expressed. Two standards, namely, fold change and P value, were used here to indicate the differential expression of the same unigene between two samples. Gene Ontology (GO) enrichment analysis of differentially expressed genes was implemented by the cluster Profiler R package, in which gene length bias was corrected. GO terms with corrected P value less than 0.05 were considered significantly enriched by differential expressed genes. KEGG is a database resource which is widely used for understanding the high-level functions and utilities of the biological system (http://www.genome.jp/kegg/). We used the cluster Profiler R package to test the statistical enrichment of differential expression genes in KEGG pathways.

Quantitative RT-PCR Analysis. *E. coli* strains were grown overnight at 37 °C in LB broth with 20 g/L glucose. Total RNA was extracted using EASYSpin Plus bacterial RNA quick extract kit (Aidlab Biotechnologies, China) according to the manufacturer's protocol. RNA concentration was detected by spectrophotometry at 260 nm. To remove the genomic DNA, samples were incubated at 42 °C for 10 min with gDNA Eraser (Takara). The RNA reverse transcription and cDNA synthesis were performed with PrimeScript RT reagent Kit. Quantitative RT-PCR was carried out using TB Green Premix Ex Taq (Takara) with the QuantStudio 1 system (Applied Biosystems). Total RNA quantity of different samples was normalized with a reference of the constitutively transcribed gene rpoD. The relative levels of mRNA were calculated using the ΔΔCt method.[36] Two independent biological samples with three technical repeats for each sample were performed for each qRT-PCR analysis. Data were the averages from two or three independent biological replicates ± the standard errors of the means.

■ ASSOCIATED CONTENT

Supporting Information

The Supporting Information is available free of charge at https://pubs.acs.org/doi/10.1021/acssynbio.9b00396.

Venn diagram and volcano plot of differentially expressed genes; oligonucleotide sequences (PDF)

■ AUTHOR INFORMATION

Corresponding Authors

Mo Xian − *CAS Key Laboratory of Biobased Materials, Qingdao Institute of Bioenergy and Bioprocess Technology, Chinese Academy of Sciences, Qingdao 266101, China*; Phone: 86-532-80662768; Email: xianmo1@qibebt.ac.cn

Guang Zhao − *CAS Key Laboratory of Biobased Materials, Qingdao Institute of Bioenergy and Bioprocess Technology, Chinese Academy of Sciences, Qingdao 266101, China*; orcid.org/0000-0003-0002-5972; Phone: 86-532-80662767; Email: zhaoguang@qibebt.ac.cn

Authors

Min Liu − *CAS Key Laboratory of Biobased Materials, Qingdao Institute of Bioenergy and Bioprocess Technology, Chinese Academy of Sciences, Qingdao 266101, China*; orcid.org/0000-0002-1305-6893

Yingxin Fu − *CAS Key Laboratory of Biobased Materials, Qingdao Institute of Bioenergy and Bioprocess Technology, Chinese Academy of Sciences, Qingdao 266101, China*

Wenjie Gao − *CAS Key Laboratory of Biobased Materials, Qingdao Institute of Bioenergy and Bioprocess Technology, Chinese Academy of Sciences, Qingdao 266101, China*

Complete contact information is available at: https://pubs.acs.org/10.1021/acssynbio.9b00396

https://dx.doi.org/10.1021/acssynbio.9b00396
ACS Synth. Biol. 2020, 9, 525−535

Author Contributions

G.Z. and M.X. developed the idea for the study. M.L. and G.Z. participated in the review of literature, and preparation of the manuscript. Y.F. and W.G. helped to establish the analytic methods and analyze the metabolites and residual glucose in the culture supernatant. L.M. did the lab work and analyzed the transcriptome results, including the plasmids and strains construction, strain cultivation, fed-batch fermentation.

Notes

The authors declare no competing financial interest.

■ ACKNOWLEDGMENTS

This work was supported by the National Defense Science and Technology Innovation Zone Foundation of China (to G.Z. and M.L.), the National Natural Science Foundation of China (31722001 and 31670089 to G.Z. and 21807101 to M.L.), the Key Program of CAS (ZDRW-ZS-2016-3M and ZDBS-SSWDQC002-03 to G.Z.) and the Natural Science Foundation of Shandong province (JQ201707 to G.Z.).

■ REFERENCES

(1) Morita, Y., Shibutani, T., Nakanishi, N., Nishikura, K., Iwai, S., and Kuraoka, I. (2013) Human endonuclease V is a ribonuclease specific for inosine-containing RNA. *Nat. Commun. 4*, 2273.

(2) Peifer, S., Barduhn, T., Zimmet, S., Volmer, D. A., Heinzle, E., and Schneider, K. (2012) Metabolic engineering of the purine biosynthetic pathway in *Corynebacterium glutamicum* results in increased intracellular pool sizes of IMP and hypoxanthine. *Microb. Cell Fact. 11*, 138.

(3) Traut, T. W. (1994) Physiological concentrations of purines and pyrimidines. *Mol. Cell. Biochem. 140*, 1−22.

(4) Cordell, R. L., Hill, S. J., Ortori, C. A., and Barrett, D. A. (2008) Quantitative profiling of nucleotides and related phosphate-containing metabolites in cultured mammalian cells by liquid chromatography tandem electrospray mass spectrometry. *J. Chromatogr. B: Anal. Technol. Biomed. Life Sci. 871*, 115−124.

(5) Ledesma-Amaro, R., Jiménez, A., Santos, M. A., and Revuelta, J. L. (2013) Biotechnological production of feed nucleotides by microbial strain improvement. *Process Biochem. 48*, 1263−1270.

(6) Ledesma-Amaro, R., Buey, R. M., and Revuelta, J. L. (2015) Increased production of inosine and guanosine by means of metabolic engineering of the purine pathway in *Ashbya gossypii*. *Microb. Cell Fact. 14*, 58.

(7) Shi, T., Wang, Y., Wang, Z., Wang, G., Liu, D., Fu, J., Chen, T., and Zhao, X. (2014) Deregulation of purine pathway in *Bacillus subtilis* and its use in riboflavin biosynthesis. *Microb. Cell Fact. 13*, 101.

(8) Asahara, T., Mori, Y., Zakataeva, N. P., Livshits, V. A., Yoshida, K.-i., and Matsuno, K. (2010) Accumulation of gene-targeted *Bacillus subtilis* mutations that enhance fermentative inosine production. *Appl. Microbiol. Biotechnol. 87*, 2195−2207.

(9) Shimaoka, M., Takenaka, Y., Kurahashi, O., Kawasaki, H., and Matsui, H. (2007) Effect of amplification of desensitized *purF* and *prs* on inosine accumulation in *Escherichia coli*. *J. Biosci. Bioeng. 103*, 255−261.

(10) Kappock, T. J., Ealick, S. E., and Stubbe, J. (2000) Modular evolution of the purine biosynthetic pathway. *Curr. Opin. Chem. Biol. 4*, 567−572.

(11) Natsumeda, Y., Prajda, N., Donohue, J. P., Glover, J. L., and Weber, G. (1984) Enzymic capacities of purine de novo and salvage pathways for nucleotide synthesis in normal and neoplastic tissues. *Cancer. Res. 44*, 2475−2479.

(12) He, B., Shiau, A., Choi, K.-Y., Zalkin, H., and Smith, J. (1990) Genes of the *Escherichia coli pur* regulon are negatively controlled by a repressor-operator interaction. *J. Bacteriol. 172*, 4555−4562.

(13) Rolfes, R. J., and Zalkin, H. (1990) Autoregulation of *Escherichia coli* purR requires two control sites downstream of the promoter. *J. Bacteriol. 172*, 5758−5766.

(14) Huffman, J. L., Lu, F., Zalkin, H., and Brennan, R. G. (2002) Role of residue 147 in the gene regulatory function of the *Escherichia coli* purine repressor. *Biochemistry 41*, 511−520.

(15) Meng, L. M., and Nygaard, P. (1990) Identification of hypoxanthine and guanine as the co-repressors for the purine regulon genes of *Escherichia coli*. *Mol. Microbiol. 4*, 2187−2192.

(16) Kim, J. H., Krahn, J. M., Tomchick, D. R., Smith, J. L., and Zalkin, H. (1996) Structure and function of the glutamine phosphoribosylpyrophosphate amidotransferase glutamine site and communication with the phosphoribosylpyrophosphate site. *J. Biol. Chem. 271*, 15549−15557.

(17) Muchmore, C. R., Krahn, J. M., Smith, J. L., Kim, J. H., and Zalkin, H. (1998) Crystal structure of glutamine phosphoribosylpyrophosphate amidotransferase from *Escherichia coli*. *Protein Sci. 7*, 39−51.

(18) Smith, J. L., Zaluzec, E. J., Wery, J.-P., Niu, L., Switzer, R. L., Zalkin, H., and Satow, Y. (1994) Structure of the allosteric regulatory enzyme of purine biosynthesis. *Science 264*, 1427−1433.

(19) Zhou, G., Smith, J., and Zalkin, H. (1994) Binding of purine nucleotides to two regulatory sites results in synergistic feedback inhibition of glutamine 5-phosphoribosylpyrophosphate amidotransferase. *J. Bio. Chem. 269*, 6784−6789.

(20) Terpe, K. (2006) Overview of bacterial expression systems for heterologous protein production: from molecular and biochemical fundamentals to commercial systems. *Appl. Microbiol. Biotechnol. 72*, 211−227.

(21) Nizam, S. A., Zhu, J., Ho, P. Y., and Shimizu, K. (2009) Effects of *arcA* and *arcB* genes knockout on the metabolism in *Escherichia coli* under aerobic condition. *Biochem. Eng. J. 44*, 240−250.

(22) Perrenoud, A., and Sauer, U. (2005) Impact of global transcriptional regulation by ArcA, ArcB, Cra, Crp, Cya, Fnr, and Mlc on glucose catabolism in *Escherichia coli*. *J. Bacteriol. 187*, 3171−3179.

(23) Saxild, H. H., and Nygaard, P. (1991) Regulation of levels of purine biosynthetic enzymes in *Bacillus subtilis*: effects of changing purine nucleotide pools. *J. Gen. Microbiol. 137*, 2387−2394.

(24) Moore, S. D. (2011) Assembling new *Escherichia coli* strains by transduction using phage P1, in *Strain Engineering*, pp 155−169, Springer.

(25) Rinas, U., Hellmuth, K., Kang, R., Seeger, A., and Schlieker, H. (1995) Entry of *Escherichia coli* into stationary phase is indicated by endogenous and exogenous accumulation of nucleobases. *Appl. Environ. Microbiol. 61*, 4147−4151.

(26) Kolter, R., Siegele, D. A., and Tormo, A. (1993) The stationary phase of the bacterial life cycle. *Annu. Rev. Microbiol. 47*, 855−874.

(27) Peifer, S., Schneider, K., Nürenberg, G., Volmer, D. A., and Heinzle, E. (2012) Quantitation of intracellular purine intermediates in different Corynebacteria using electrospray LC-MS/MS. *Anal. Bioanal. Chem. 404*, 2295−2305.

(28) Liu, M., Feng, X., Ding, Y., Zhao, G., Liu, H., and Xian, M. (2015) Metabolic engineering of *Escherichia coli* to improve recombinant protein production. *Appl. Microbiol. Biotechnol. 99*, 10367−10377.

(29) Farmer, W. R., and Liao, J. C. (1997) Reduction of aerobic acetate production by *Escherichia coli*. *Appl. Environ. Microbiol. 63*, 3205−3210.

(30) Kumari, S., Beatty, C. M., Browning, D. F., Busby, S. J., Simel, E. J., Hovel-Miner, G., and Wolfe, A. J. (2000) Regulation of acetyl coenzyme A synthetase in *Escherichia coli*. *J. Bacteriol. 182*, 4173−4179.

(31) Liu, M., Yao, L., Xian, M., Ding, Y., Liu, H., and Zhao, G. (2016) Deletion of *arcA* increased the production of acetyl-CoA-derived chemicals in recombinant *Escherichia coli*. *Biotechnol. Lett. 38*, 97−101.

(32) Phue, J. N., Noronha, S. B., Hattacharyya, R., Wolfe, A. J., and Shiloach, J. (2005) Glucose metabolism at high density growth of *E. coli* B and *E. coli* K: differences in metabolic pathways are responsible for efficient glucose utilization in *E. coli* B as determined by

https://dx.doi.org/10.1021/acssynbio.9b00396
ACS Synth. Biol. 2020, 9, 525−535

microarrays and Northern blot analyses. *Biotechnol. Bioeng. 90*, 805−820.
(33) Yoon, S. H., Jeong, H., Kwon, S.-K., and Kim, J. F. (2009) Genomics, biological features, and biotechnological applications of *Escherichia coli* B:"Is B for better?!, in *Systems Biology and Biotechnology of Escherichia coli*, pp 1−17, Springer.
(34) Liu, M., Tolstorukov, M., Zhurkin, V., Garges, S., and Adhya, S. (2004) A mutant spacer sequence between-35 and-10 elements makes the Plac promoter hyperactive and cAMP receptor protein-independent. *Proc. Natl. Acad. Sci. U. S. A. 101*, 6911−6916.
(35) Baba, T., Ara, T., Hasegawa, M., Takai, Y., Okumura, Y., Baba, M., Datsenko, K. A., Tomita, M., Wanner, B. L., and Mori, H. (2006) Construction of *Escherichia coli* K-12 in-frame, single-gene knockout mutants: the Keio collection. *Mol. Syst. Biol. 2*, 8−19.
(36) Livak, K., and Schmittgen, T. (2001) Analysis of relative gene expression data using real-time quantitative PCR and the 2-$^{\triangle\triangle}$Ct method. *Methods 25*, 402−408.

https://dx.doi.org/10.1021/acssynbio.9b00396
ACS Synth. Biol. 2020, 9, 525−535